RESEARCH PAPER

Hydrothermal synthesis and characterization of $Tb_xPb_{1-x}Te$ nanomaterials: physical and optical properties

Younes Hanifehpour *

Department of Chemistry, Sayyed Jamaleddin Asadabadi University, Asadabad, Iran

ARTICLE INFO

Article History:
Received 03 July 2020
Accepted 17 September 2020
Published 15 October 2020

Keywords:
Terbium
PbTe
Electrical conductivity
Nanomaterial
Hydrothermal

ABSTRACT

In this study, Tb-doped PbTe nanoparticles with variable Tb3+ content were synthesized by a simple hydrothermal technique. The synthesized nanoparticles were characterized by X-ray photoelectron spectroscopy (XPS), scanning electron microscopy (SEM), and powder X-ray diffraction (XRD). The XRD patterns indicated that the particles were excellently crystallized due to the cubic PbTe phase. The SEM images certify that the substitution of Tb into the lattice of PbTe does not change the morphology of PbTe nanoparticles. The SEM images displayed that the size of the particles was in the range of 25-80 nm. The energy of the bandgap of doped-PbTe and PbTe nanoparticles expected from the chief absorption edges of the UV-Vis diffuse reflectance spectrum. Blue shifts in DRS spectra of PbTe were noticed by increasing the concentration of the Tb3+ ions. The incorporation of Tb^{3+} into the PbTe lattice was confirmed by the XPS technique. The electrical conductance of various Tb-doped PbTe samples is higher than that for the pure PbTe, and elevates with temperature.

How to cite this article
Hanifehpour Y. Hydrothermal synthesis and characterization of $Tb_xPb_{1-x}Te$ nanomaterials: physical and optical properties. Nanochem Res, 2020; 5(2):241-248. DOI: 10.22036/ncr.2020.02.014

INTRODUCTION

Much consideration has been paid to IV–VI Pb chalcogenide for application in thermoelectric (TE) devices, solar cells, telecommunication, photodetectors, field-effect transistors (FET) and photovoltaics. The chalcogenide of Pb with many conventional II–VI and III–V compounds have narrower band-gaps and larger Bohr radius [1]. PbTe as a member of the lead chalcogenide family is a favored thermoelectric material; this is one of the first materials studied by Ioffe and his colleagues in the middle of the last century [2]. This material has achieved great attention because of its high mobility, small bandgap (0.31 eV at 300 K) , high dielectric constant, and face-centered cubic structure . In comparison to other semiconductor compounds, the Quantum size effect can be noticed in the large size structures due to the large exciton Bohr radius of lead telluride (46nm) [3-5].

* Corresponding Author Email: *hanifehpour@gmail.com*

Rare earth-incorporated nanomaterials with diverse compositions have become an increasingly vital in various fields, such as light-emitting displays, novel photocatalist, luminescent devices, biological labeling, and imaging [6-11], due to the introduction of dopant levels within the bandgap and qualification of the band structure. However, some studies have been carried out on doped-PbTe with some lanthanides to improve its optical and thermoelectric properties [12,13], whereas there is no report of doping of PbTe with Terbium(Tb) as a lanthanide ion. The substitution of large electropositive cations like lanthanides atoms (i.e., Tb) into PbTe lattice could be expected to influence its electronic, physical and electrical properties. Here, we report the preparation, structural, electrical, and optical properties of Tb^{+3}-doped lead telluride via co-reduction route at the hydrothermal process.

EXPERIMENTAL DETAILS

Materials

The chemicals utilized in this work had analytical grades and utilized with no further purification. $Pb(NO_3)_2$ (99%) was purchased from Kanto chemical company and Tb $(NO_3)_3.5H_2O$, sodium hydroxide (NaOH 98%), sodium borohydride ($NaBH_4$ 98%), ethanol (99%), and sodium tellurite (Na_2TeO_3 100mesh 99%) were obtained from Sigma-Aldrich.

Synthesis of PbTe and Tb-Doped PbTe Samples

Tb-doped lead selenide compounds with different Tb contents (0–12 mol%) were prepaired hydrothermally utilizing sodium borohydride ($NaBH_4$ 98%), as a reducing agent. Within a characteristic synthesis, proper stoichiometric $Pb(NO3)_2$ (1 mmol), Na_2TeO_3 powders(1mmol), Tb $(NO_3)_3.5H_2O$ (1mmol), and NaOH (0.05g) were added to 40 mL of distilled water in a beaker, and the mixture was dispersed to form a deposition by constant stirring. Afterward, 0.3 g $NaBH_4$ was put into the beaker after the solution changed to purple-black and being stirred for 15 min. The mixture was transferred into A 100 mL stainless Teflon-lined autoclave and maintained at 220 °C for 18 h and then cooled to room temperature naturally. Finally, as-prepared samples were washed with absolute alcohol and distilled-water twice to eliminate residual impurities and then dried at 50 °C for 12 h. As a result, the black powders were acquired.

Characterization Instruments

The XRD diffraction patterns of the prepared products were recorded on D8 Advance, Bruker (Germany), diffractometer with monochromatic high-intensity Cu Ka radiation (l = 1.5406 Å), an accelerating voltage of 40 kV, and an emission current of 30 mA. SEM (S- 4200, Hitachi, Japan) was utilized to perceive morphology and the surface state of the obtained nanoparticles. Four-point probe technique was employed for the measurement of thermoelectrical and electrical resistivity of materials. A small oven was required for the temperature variation of the samples from the room temperature to about 200°C (maximum). A small chip with 7-mm length and 1-mm thickness was used for this test. The absorption spectra were recorded with UV–Vis spectrophotometer (Varian Cary 3 Bio). Chemical states and chemical compositions of the samples were carried out through X-ray photoelectron spectroscopy (XPS) (Model: K-ALPHA, UK).

RESULTS AND DISCUSSION

Fig. 1 displays the XRD patterns of $Tb_{1-x}Pb_xTe$ and pure PbTe nanoparticles. The sharp and strong peaks implied that the samples are well crystallized. All the diffraction peaks can be attributed to the cubic phase of PbTe (JCPDF: 78-1905) [14]. No

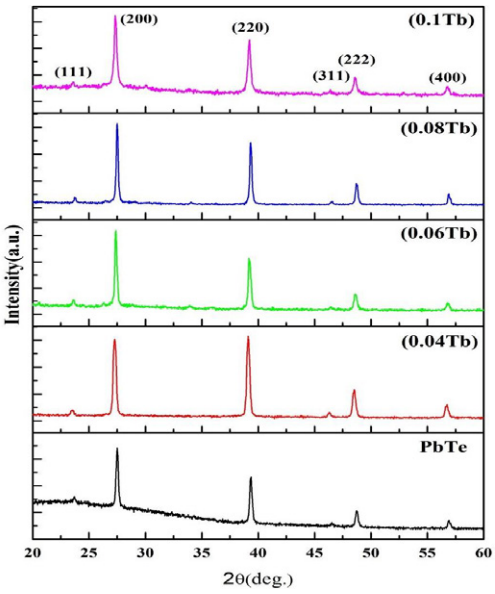

Fig. 1. XRD pattern of prepared PbTe and Tb-doped PbTe nanoparticle

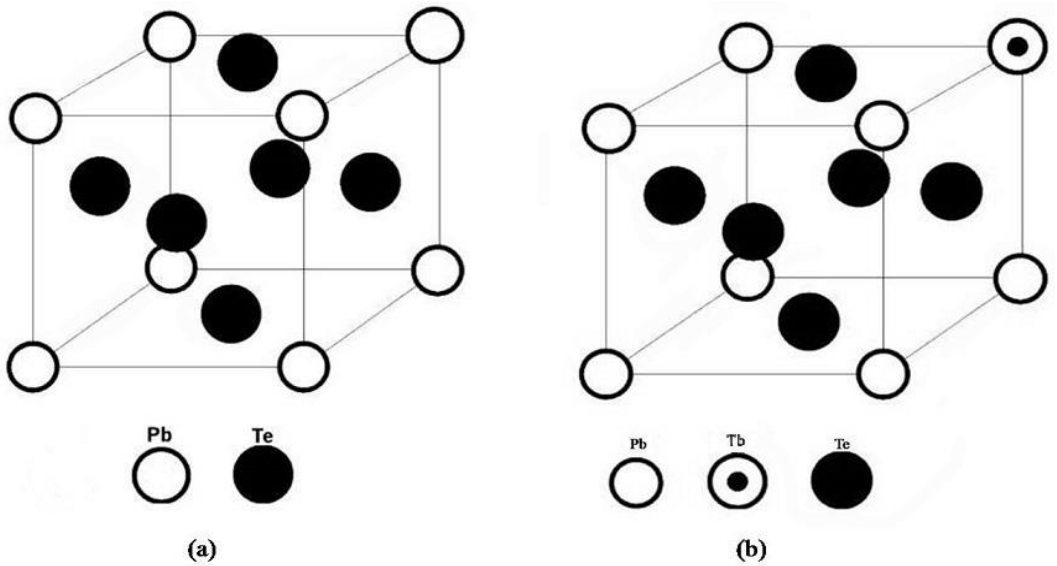

Fig. 2. (a)The lattice of PbTe as NaCl type. For example (b) Tb is presented as a doping impurity ion into the Pb sublattice.

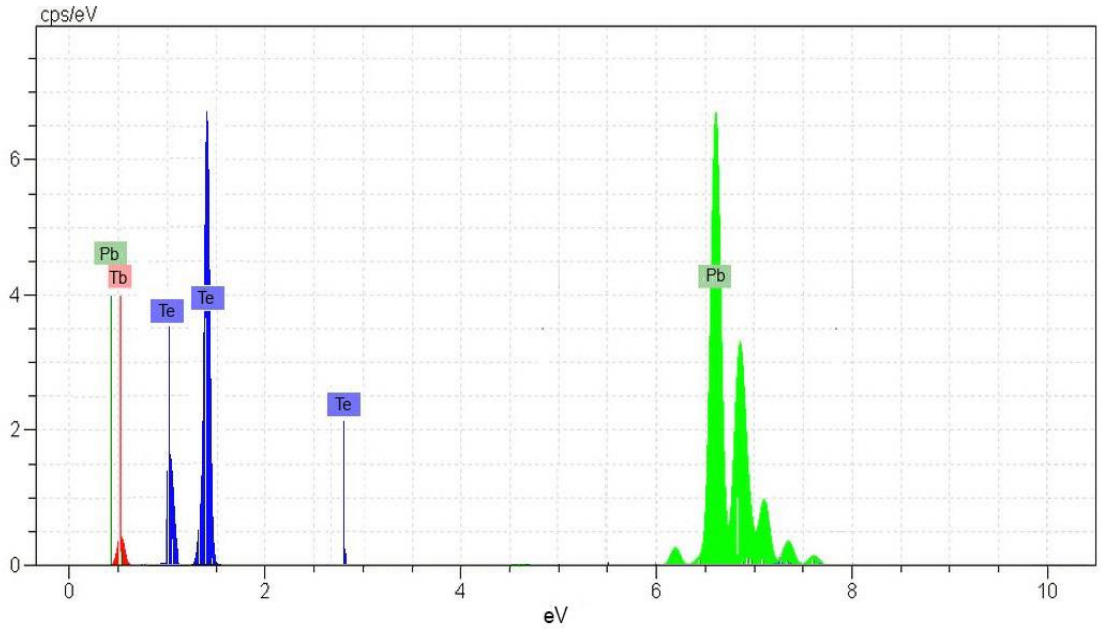

Fig. 3. EDX analysis of the as-synthesized 8% Tb-doped PbTe nanomaterials.

peaks corresponding to other impurities Tb_2O_3 phase were noticed in the pattern, depicting that Tb was completely doped into the PbTe crystal lattice (Fig.2.). From the X-ray diagram, it is also realized that there is no variation in peak positions for the doped-compounds. This indicates that the doped-PbTe and pure systems have the same crystal symmetry. Therefor, all these samples display a similar basic XRD pattern.

The EDS spectrum of the product was employed to further confirm the formation, chemical composition, and purity of as-synthesized Tb-PbTe nanoparticles. The EDX pattern of 8% Tb-doped PbTe is shown in Fig. 3 and shows that only Pb, Tb and Te elements are present. The molar ratio of Pb/Tb to Te is almost 1:1, which is almost consistent with stoichiometric PbTe. Therefore, both XRD and EDX analyses show that pure Tb-doped PbTe

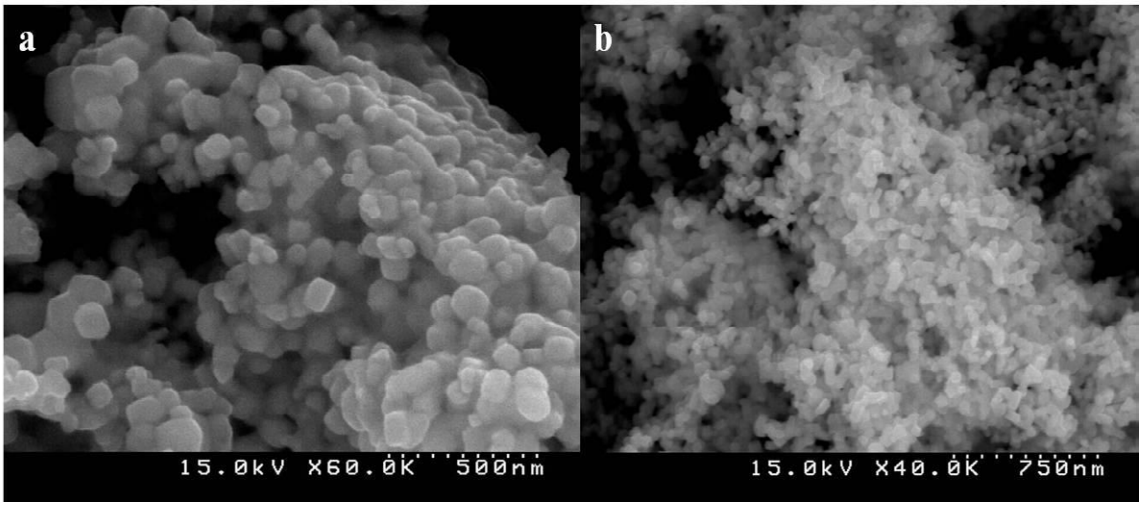

Fig. 4. SEM images of PbTe at two different magnification.

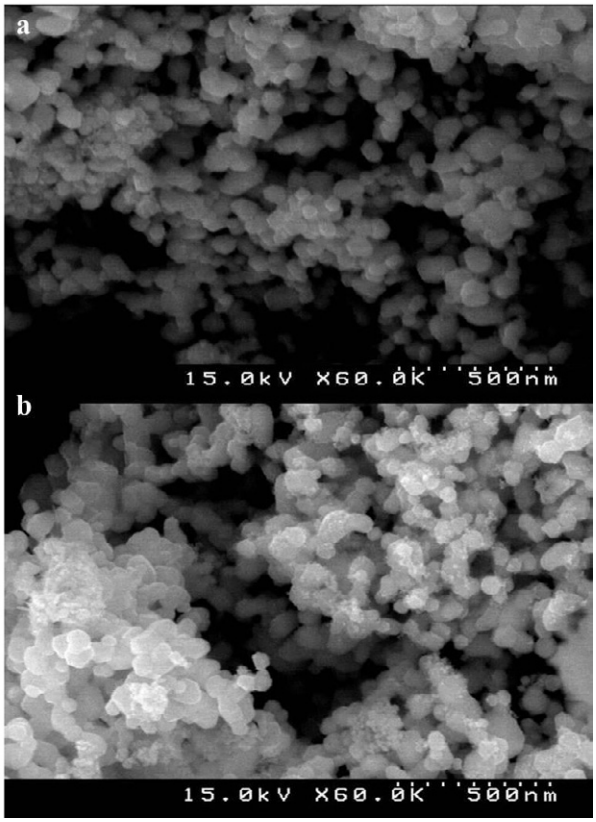

Fig. 5.SEM images of a) $Tb_{0.04}Pb_{0.96}Te$ and b)$Tb_{0.1}Pb_{0.9}Te$ nanoparticles synthesized in 220°C for 18h.

compounds are successfully produced via the present synthetic route.

Fig. 4 shows the SEM images of PbTe produced by hydrothermal approach at two different magnifications and depicts that the sample is composed of homogenous nanocubes. Many nanocuboids could be clearly found. The average size of particles was 55nm.

Fig. 5 shows the SEM microphotographs of the Tb-doped PbTe samples, respectively. As seen, there are consistent nanometer-scale particles with good size distribution in all cases and the

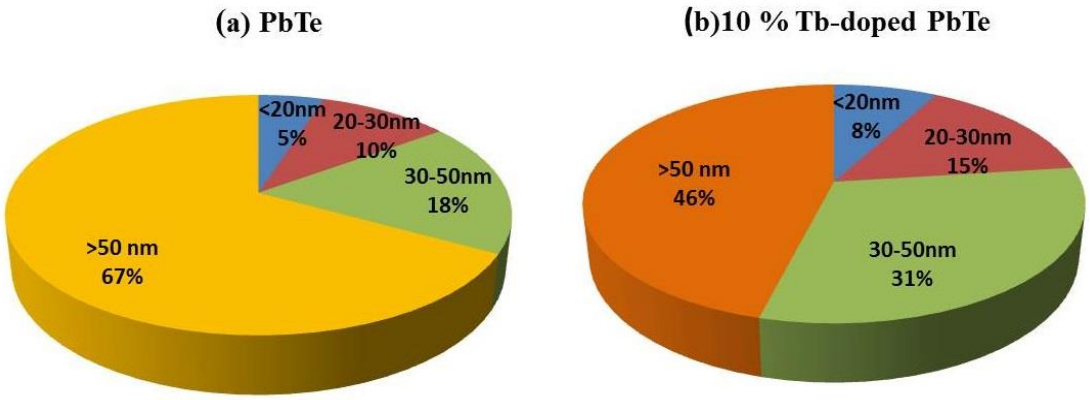

Fig. 6. Particle size distribution of a) pure PbTe and b) $Tb_{0.1}Pb_{0.90}Te$ nano particles.

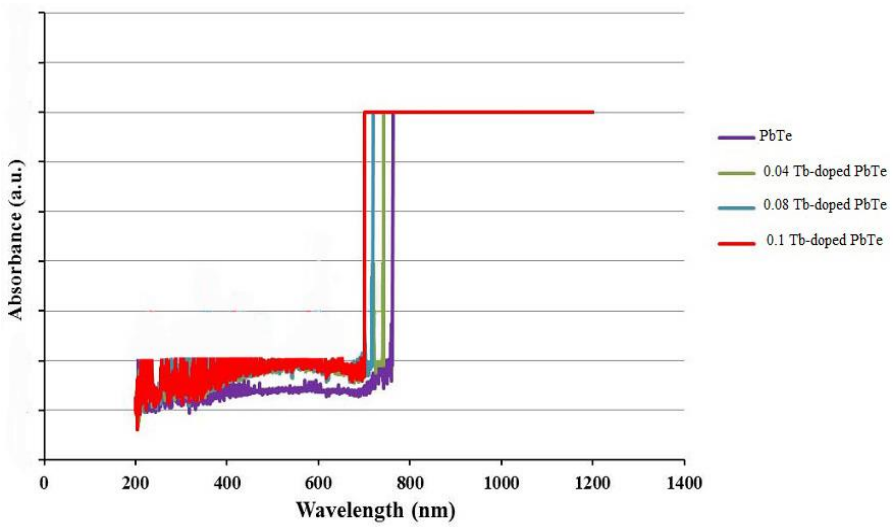

Fig. 7. UV/Vis Absorption measurments for PbTe and with different molar concentration of Tb as dopant.

as-prepared product displays cubic morphology with a narrow size distribution of 15-80 nm. These figures certify that the substitution of Tb into the lattice of PbTe does not change the morphology of PbTe nanoparticles. The SEM images of doped compounds showed that the samples were uniforms with dopants (Tb) substituting Pb sites in the PbTe compound and do not contain any other dopant dominating phases.

In order to further evaluate, size distribution histograms of these nano-particles has been obtained through Manual Microstructure Distance Measurement program. Figs. 6a–b show the distribution size histograms of as-synthesized materials, respectively. The particles are uniform and they have a narrow range of distribution. The particle size in doped samples is smaller than pure one according to the size distribution diagram.

The UV-Vis diffuse reflectance spectra were utilized for the evaluation of the photophysical properties of the as-obtained nanoparticles. Absorption of light by the semiconductor depends on the gap between the valence and conduction band, and the impurity dosage in the host lattice [15]. The DRS spectra of bare and Tb-doped lead telluride are presented in Fig. 7. The reflectance characteristics of the doped PbTe sample were quite similar to that of the undoped sample. It can be seen that the all samples displayed a strong photoabsorption at the visible light range. There is a blue shift in absorbance spectra of Tb-doped PbTe compared to PbTe, as not anticipated for doped-

Table 1. Absorption edges for $Ln_xPb_{1-x}Te$ compounds

material	E_g(eV)
PbTe	1.621
$Tb_{0.04}Pb_{0.96}Te$	1.645
$Tb_{0.08}Pb_{0.092}Te$	1.679
$Tb_{0.1}Pb_{0.9}Te$	1.689

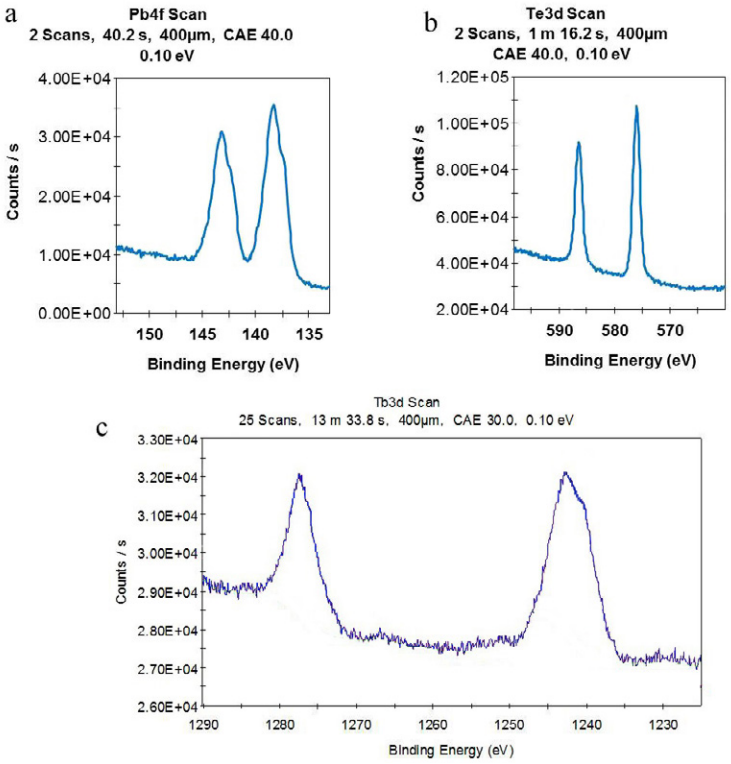

Fig. 8. XPS spectra of 4 % Tb-doped PbTe nanomaterials.

materials. The electronic properties of lead telluride could be affected by doping of lanthanide ions into a Pb–Te framework. Introducing Lanthanide cations into PbTe lattice results in changing of Pb -Te bond and increase of bandgap. As obviously seen in Fig. 7, as the impurity dosage elevates, a shift in the absorption edge towards higher energy occurs. The increase in bandgap with carrier concentration can be explained on the basis of Burstein–Moss effect. As the doping level increases ,electrons from the valence band have to transit to the electron states higher than those occupied by donor electrons near the conduction band edge [16]. The blue shift in the absorption edge also confirms the fact that Lanthanide cations play as a donor in the PbTe host .

The energy of the bandgap of doped-PbTe and PbTe nanoparticles expected from the chief absorption edges of the UV-Vis diffuse reflectance spectrum. Band gap energy is provided in Table 1.The band gap indicates an increase with dopant dosage from 0.00 M to 0.1M.

X-ray photoelectron spectroscopy (XPS) analysis of 4% Tb-doped PbTe nanoparticles was carried out to certify substitution of Tb into the PbTe lattice and to determine the oxidation state of Tb in the PbTe lattice. The XPS spectra of 4% Tb-doped PbTe nanoparticles are presented in Fig. 7. The high-resolution spectrum of Pb4f in Fig. 8a shows two peaks for Pb $4f_{5/2}$ (143.1 eV) and $Pb4f_{7/2}$ (138.3 eV), respectively, supporting the existence of Pb^{2+} [17]. As shown in Fig.8b, the binding energies for $Te3d_{5/2}$ and $Te3d_{3/2}$ are 575.7 eV and 586.2 eV, respectively. The observed values for the binding energies are close to the reported value of Te^{2-}[18]. As shown in Fig. 8c, the Tb 3d peaks placed at 1275.97 and 1244.25 eV confirm that Tb ions have

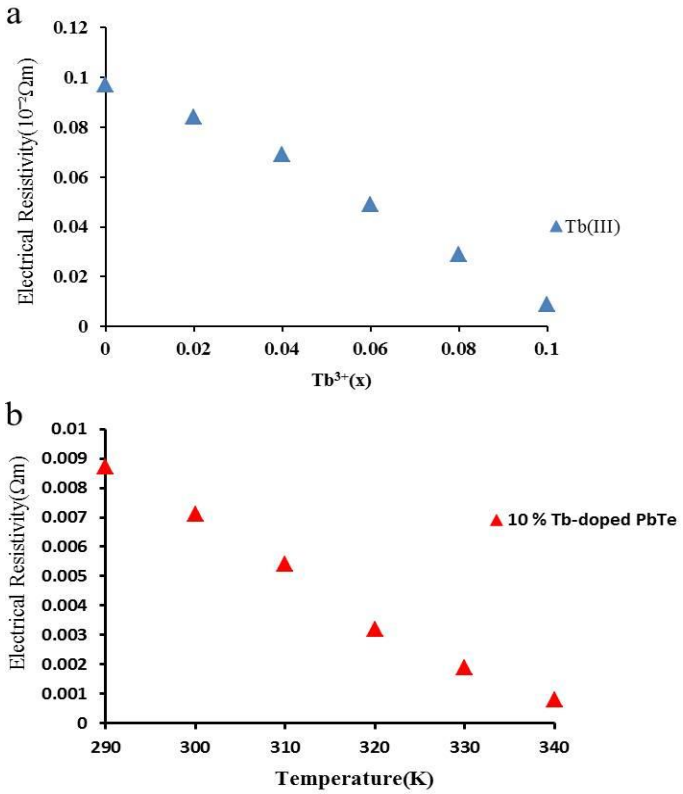

Fig. 9.(a) electrical and (b)thermoelectrical resistivity of $Tb_xPb_{1-x}Te$ compounds.

been doped successfully into the PbTe's crystal lattice [19].

The four-probe technique was employed for the measurement of electrical and thermoelectrical resistivity of samples. Fig. 9a shows the electrical resistivity of Tb-doped PbTe nanomaterials. The electrical resistivity measured at room temperature for pure PbTe was of the order of 0.09×10^{-2} Ω.m. The minimum value of electrical resistivity for Tb^{3+}-doped compounds is 0.087×10^{-2} Ωm. Fig. 9b shows the temperature dependence of the electrical resistivity for Tb-doped PbTe between 290 and 340 K in which the electrical resistivity decreases with temperature. The lowest value of electrical resistivity for $Tb_{0.1}Pb_{0.9}Te$ is 0.0009×10^{-2} Ωm. Subsequently, the electrical conductance of Tb-doped PbTe materials is higher than that of undoped PbTe at RT and elevates with temperature.

COCLUSION

In this study, an efficient and simple hydro-thermal approach was applied for preparation of Tb-doped PbTe and cuboid PbTe, as a thermo-electric compound via using $NaBH_4$, $Pb(NO_3)_2$, NaOH ,Na_2TeO_3, and H_2O as the starting materials. The XPS, XRD, SEM and TEM analyses results have supported that the substituting of Tb ions into PbTe lattice change neither the the morphology nor crystal nature of PbTe nanoparticles. In this paper, we have shown a series of Tb- doped PbTe samples indicating that a gap increase, up to 0.10 eV, occuring at the highest doping levels, is required to thermoelectrics.The electrical conductance of Tb-doped PbTe is higher than that of pure PbTe and increases with temperature.

ACKNOWLEDGMENT

The author gratefully acknowledge the Sayyed Jamaleddin Asadabadi University for providing support to this work.

CONFLICT OF INTEREST

The authors declare that there are no conflicts of interest.

REFERENCES

1. Lin Z, Wang M, Wei L, Song X, Xue Y, Yao X. PbTe colloidal nanocrystals: Synthesis, mechanism and infrared optical characteristics. Journal of Alloys and Compounds. 2011;509(16):5047-9.

2. Ahmad S, Mahanti SD, Hoang K, Kanatzidis MG. Ab initiostudies of the electronic structure of defects in PbTe. Physical Review B. 2006;74(15).
3. Wang C, Zhang G, Fan S, Li Y. Hydrothermal synthesis of PbSe, PbTe semiconductor nanocrystals. Journal of Physics and Chemistry of Solids. 2001;62(11):1957-60.
4. Lukovic D, Nikolic PM, Vujatovic S, Savic S, Urosevic D. Photoacoustic properties of single crystal PbTe(Ni). Science of Sintering. 2007;39(2):161-7.
5. Zong Z, Wang H, Kong L. Assembly of PbTe/Pb-based nanocomposite and photoelectric property. Nanoscale Research Letters. 2013;8(1):191.
6. Hanifehpour Y, Joo SW, Min B-K. Lu3+/Yb3+ and Lu3+/Er3+ co-doped antimony selenide nanomaterials: synthesis, characterization, and electrical, thermoelectrical, and optical properties. Nanoscale Research Letters. 2013;8(1).
7. Alemi A, Hanifehpour Y, Joo SW, Khandar A, Morsali A, Min B-K. Synthesis and characterization of new LnxSb2−xSe3 (Ln: Yb3+, Er3+) nanoflowers and their physical properties. Physica B: Condensed Matter. 2012;407(1):38-43.
8. Hamnabard N, Hanifehpour Y, Khomami B, Woo Joo S. Synthesis, characterization and photocatalytic performance of Yb-doped CdTe nanoparticles. Materials Letters. 2015;145:253-7.
9. Alemi A, Klein A, Meyer G, Dolatyari M, Babalou A. Synthesis of New LnxBi2-xSe3 (Ln: Sm3+, Eu3+, Gd3+, Tb3+) Nanomaterials and Investigation of Their Optical Properties. Zeitschrift für anorganische und allgemeine Chemie. 2010;637(1):87-93.
10. Alemi A, Hanifehpour Y, Joo SW, Min B-K. Synthesis of novel LnxSb2−xSe3 (Ln: Lu3+, Ho3+, Nd3+) nanomaterials via co-reduction method and investigation of their physical properties. Colloids and Surfaces A: Physicochemical and Engineering Aspects. 2011;390(1-3):142-8.
11. Hanifehpour Y, Soltani B, Amani-Ghadim AR, Hedayati B, Khomami B, Joo SW. Synthesis and characterization of samarium-doped ZnS nanoparticles: A novel visible light responsive photocatalyst. Materials Research Bulletin. 2016;76:411-21.
12. Dashevsky Z, Shusterman S, Dariel MP, Drabkin I. Thermoelectric efficiency in graded indium-doped PbTe crystals. Journal of Applied Physics. 2002;92(3):1425-30.
13. Akhmedova GA, Abdinov DS. Effect of thallium doping on the thermal conductivity of PbTe single crystals. Inorganic Materials. 2009;45(8):854-8.
14. Zlatanov ZK. Mechanical properties and structure of Gd-doped PbTe. Materials Chemistry and Physics. 2007;103(2-3):470-4.
15. Nouneh K, Plucinski KJ, Bakasse M, Kityk IV. Thermoelectrical properties and optical third harmonic generation of Gd-doped PbTe. Journal of Materials Science. 2007;42(16):6847-53.
16. Sharma G, Chawla P, Lochab SP, Singh N. Burstein Moss effect in nanocrystalline CaS : Ce. Bulletin of Materials Science. 2011;34(4):673-6.
17. Zhao W, Ge P-Y, Xu J-J, Chen H-Y. Catalytic Deposition of Pb on Regenerated Gold Nanofilm Surface and Its Application in Selective Determination of Pb2+. Langmuir. 2007;23(16):8597-601.
18. Li G-R, Yao C-Z, Lu X-H, Zheng F-L, Feng Z-P, Yu X-L, et al. Facile and Efficient Electrochemical Synthesis of PbTe Dendritic Structures. Chemistry of Materials. 2008;20(10):3306-14.
19. Shi M, Zeng C, Wang L, Nie Z, Zhao Y, Zhong S. Straw-sheaf-like terbium-based coordination polymer architectures: microwave-assisted synthesis and their application as selective luminescent probes for heavy metal ions. New Journal of Chemistry. 2015;39(4):2973-9.